

Importance of Prolate Neutrino Radiation in Core-Collapse Supernovae: The Reason for the Prolate Geometry of SN1987A?

Hideki MADOKORO, Tetsuya SHIMIZU, and Yuko MOTIZUKI
RIKEN, 2-1 Hirosawa, Wako, Saitama 351-0198
madokoro@postman.riken.jp, tss@postman.riken.jp, motizuki@riken.jp

(Received 2003 December 26; accepted 2004 May 25)

Abstract

We have carried out 2-D simulations of core-collapse supernova explosions. The local neutrino radiation field was assumed to have its maximum value either at the symmetry (polar) axis or on the equatorial plane. These led to prolate and oblate explosions, respectively. We have found that the gain of the explosion energy in the prolate explosion evolves more predominately than that in the oblate one when the total neutrino luminosity is given. Namely, the prolate explosion is more energetic than the oblate one.

One of the authors (Shimizu et al. 2001) showed for the first time that globally anisotropic neutrino radiation produces a more powerful explosion than does spherical neutrino radiation. In our previous study (Madokoro et al. 2003), we improved the numerical code of Shimizu et al. (2001), and demonstrated that globally anisotropic neutrino radiation yields a more energetic explosion than does spatially-fluctuated neutrino radiation. Together with the result of this paper, we conclude that globally anisotropic (prolate) neutrino radiation is the most effective way to increase the explosion energy among various types of explosions investigated in these studies. We discuss the reason for this. Our result is suggestive of the fact that the expanding materials of SN1987A have been observed to have a prolate geometry.

Key words: hydrodynamics — shock waves — stars: neutron — stars: supernovae: general — stars: supernovae: individual (SN1987A)

1. Introduction

An aspherical explosion is one of the key issues in studying core-collapse supernovae. Observations have suggested that the spherical symmetry is broken in several supernova explosions. For example, speckle and spectropolarimetry observations have shown that the spectra of core-collapse supernovae are significantly polarized at a level of 0.5 to 4% (Méndez et al. 1988; Jeffery 1991; Wang et al. 1996, 2001; Leonard et al. 2000; Höflich et al. 2003). Recent Hubble Space Telescope images and spectroscopy have revealed that SN1987A has an axially symmetric geometry (Wang et al. 2002). Wang et al. (2002) also reported that the polarization represents a prolate geometry that has been fixed in time. They discussed that a jet-driven model based on asymmetry associated with neutrino flow (Shimizu et al. 1994, 2001; Fryer, Heger 2000) may account for the observed asymmetries of SN1987A. Large values of observed pulsar kicks ($> 400 \text{ km s}^{-1}$; see, e.g., Fryer et al. 1998) are also a manifestation of asymmetry. Furthermore, it has been theoretically demonstrated that most of simulations assuming spherical symmetry fail to yield robust explosions (e.g., Liebendörfer et al. 2001). These facts necessarily lead us to multi-dimensional simulations.

Several groups have performed 2-D and 3-D simulations. It was shown (Miller et al. 1993; Herant et al. 1994; Burrows et al. 1995; Janka, Müller 1996; Mezzacappa et al. 1998; Fryer, Heger 2000; Fryer, Warren 2002; Kifonidis et al. 2003) that convection in the neutrino-heated region behind the supernova shock or inside a nascent neutron star plays an important role to increase the explosion energy.

Some groups also noticed the role of anisotropic neutrino emission from a protoneutron star. Janka and Mönchmeyer (1989a, 1989b) carried out 2-D simulations with rotation in order to explain the observed properties of SN1987A. When a protoneutron star rotates, centrifugal force will deform the core into an oblate form, and hence the neutrino flux distribution will preferentially be concentrated on the rotational (polar) axis. They concluded that the neutrino flux along the rotational axis could become up to three-times larger than that on the equatorial plane. Later, Keil, Janka, and Müller (1996) performed 2-D simulations without rotation, but taking into account the convection inside the protoneutron star (Ledoux convection). They found that the neutrino flux on the surface of a protoneutron star shows a fluctuated anisotropy of $\sim 3\text{--}4\%$. Recently, Kotake, Yamada, and Sato (2003) performed simulations of the rotational core-collapse, and obtained anisotropic neutrino heating, depending on their initial model with the degree of anisotropy in the neutrino heating rate from close to unity to more than a factor of 10.

Shimizu, Yamada, and Sato (1994) and Shimizu et al. (2001) performed a series of systematic 2-D simulations in order to study the effects of anisotropic neutrino radiation on the explosion mechanism, itself. They found that, when the total neutrino luminosity is given, only a few percent of enhancement in the neutrino flux along the axis of symmetry is sufficient to increase the explosion energy by a large factor. They also found that this effect saturates around a certain degree of anisotropy. Furthermore, it was found that the effect of anisotropic neutrino radiation becomes more prominent when the total neutrino luminosity is low, while the

difference between the anisotropic and spherical models diminishes significantly if the total neutrino luminosity is sufficiently high. Note that they proposed rotation as one of the origins of anisotropic neutrino radiation; anisotropy in neutrino radiation may also originate from convection inside a nascent neutron star, or asymmetric mass accretion onto a protoneutron star.

Shimizu et al. (2001) considered only the case in which the maximum value in the neutrino flux distribution was located at the axis of symmetry. Janka and Keil (1998), however, pointed out that the neutrino flux can also be peaked on the equatorial plane. Following their previous study (Keil et al. 1996), they carried out 2-D simulations with both rotation and convection above and inside a nascent neutron star. It was found, at a very early phase of neutrino emission, that the neutrino flux was peaked at the rotational axis. However, they found that at a later stage of evolution Ledoux convection occurs strongly on the equatorial plane, while being suppressed near to the rotational axis due to a combination effect of centrifugal force and convection. Consequently, the neutrino flux on the equatorial plane was enhanced over that along the rotational axis.

In this paper, we consider the effects of oblate neutrino heating, suggested by Janka and Keil (1998), on the explosion dynamics. We focus on the shock position, the explosion energy, and asymmetric explosions. Our purpose in this article, which follows that of previous studies (Shimizu et al. 2001; Madokoro et al. 2003), is to understand what kind of neutrino radiation is favorable for a successful explosion through a parameter study when the total neutrino luminosity is given.

This paper is organized as follows. In section 2, we describe our numerical simulation. We then discuss our numerical results in section 3. The results of an oblate explosion are compared with those of a prolate one. We find that locally intense neutrino heating along the pole, which leads to a prolate explosion, is a more effective way to increase the explosion energy than oblate heating when the total neutrino luminosity is given. Finally, a brief summary is presented in section 4.

2. Numerical Simulation

We performed 2-D simulations by solving hydrodynamical equations in spherical coordinates (r, θ) . A generalized Roe's method was used to solve the general equations of motion. Our computational region ranged from 50 km to 10000 km in radius from the center of the protoneutron star. We started our calculations when a stalled shock wave was formed at ~ 200 km. The temperature on the neutrinosphere, T_ν , and the total neutrino luminosity, L_ν , were assumed to be constant in our simulations. The details of our numerical technique, the EOS, and the initial condition are described in Shimizu et al. (2001).

We obtained the initially stalled shock by solving stationary hydrodynamic equations with assuming spherical symmetry. For the purpose of this study, this assumption was sufficient. Note that in a simulation model by another group (Kotake et al. 2003), the stalled shock wave can become almost spherical, even if the protoneutron star rotates with the rotational velocity, which the authors call 'moderate' (and with weak differential rotation). We stopped our calculations with a constant L_ν at $t = 500$ ms after shock stagnation. This is because recent one- and two-dimensional simulations have shown that the

timescale of decay of the neutrino luminosity after the shock stall is about 500 ms (Bruenn 1993; Woosley et al. 1994; Janka, Müller 1995; Fryer, Heger 2000).

We fixed the radius of the protoneutron star, R_{NS} , to be 50 km in our simulation. The neutrinosphere actually shrinks as a result of neutrino emission (Burrows et al. 1995). However, the effect of shrinking of the neutrinosphere was not important in our present study. The reasons are as follows: Firstly, the degree of anisotropy in the neutrino radiation at a distant point from the neutrinosphere (which we denote ' c_2 ') depends strongly on the degree of anisotropy on the neutrinosphere (denoted by ' a '), while it is insensitive to R_{NS} [see equation (8) later]. Secondly, the region in which we are interested is 1000 km above the neutrinosphere. We thus expect that a small change of the radius of the neutrinosphere (from 50 km to 40 km; see Burrows et al. 1995) does not affect the shock dynamics qualitatively during a timescale of 500 ms on which we simulated. Thirdly, we fixed both the radius of the protoneutron star and the neutrino energy (or equivalently the neutrino temperature) in our simulation. On the other hand, the neutrinosphere actually shrinks as a result of neutrino emission, while at the same time the neutrino energy increases. It is therefore a good approximation to consider that the rate of absorption of the neutrino energy on the shocked matter is approximately constant during the short timescale of 500 ms. We then think that the qualitative result is the same as our present result, even if we include both the shrinking of the protoneutron star and the increase of the neutrino energy.

We improved (Madokoro et al. 2003) the numerical code of Shimizu et al. (2001): the cells in the θ -direction were shifted by half of the cell size (Shimizu 1995) in order to avoid a numerical error near the pole. Note that this numerical error was not serious, and only minor for the investigation of the explosion energy, but may affect the results of nucleosynthesis.

The local neutrino flux is assumed to be

$$l_\nu(r, \theta) = \frac{7}{16} \sigma T_\nu^4 c_1 (1 + c_2 \cos^2 \theta) \frac{1}{r^2}, \quad (1)$$

where σ is the Stefan-Boltzmann constant. In equation (1), c_2 is a parameter which is related to the degree of anisotropy in the neutrino radiation at a distant point far from the neutrinosphere. In order to see the effect of anisotropic neutrino radiation, itself, on the explosion, the value of c_1 was calculated from the given c_2 so as to adjust the total neutrino luminosity to that in the spherical model at the same T_ν . The total neutrino luminosity was obtained by integrating equation (1) over the whole solid angle,

$$L_\nu = \int r^2 l_\nu(r, \theta) d\Omega = \frac{7}{16} \sigma T_\nu^4 4\pi c_1 \left(1 + \frac{1}{3} c_2\right), \quad (2)$$

which is equated to that of a spherical explosion with the same T_ν ,

$$L_\nu^{\text{sp}} = \frac{7}{16} \sigma T_\nu^4 4\pi R_{\text{NS}}^2. \quad (3)$$

By comparing equations (2) with (3), we obtain

$$c_1 = \frac{R_{\text{NS}}^2}{1 + c_2/3}. \quad (4)$$

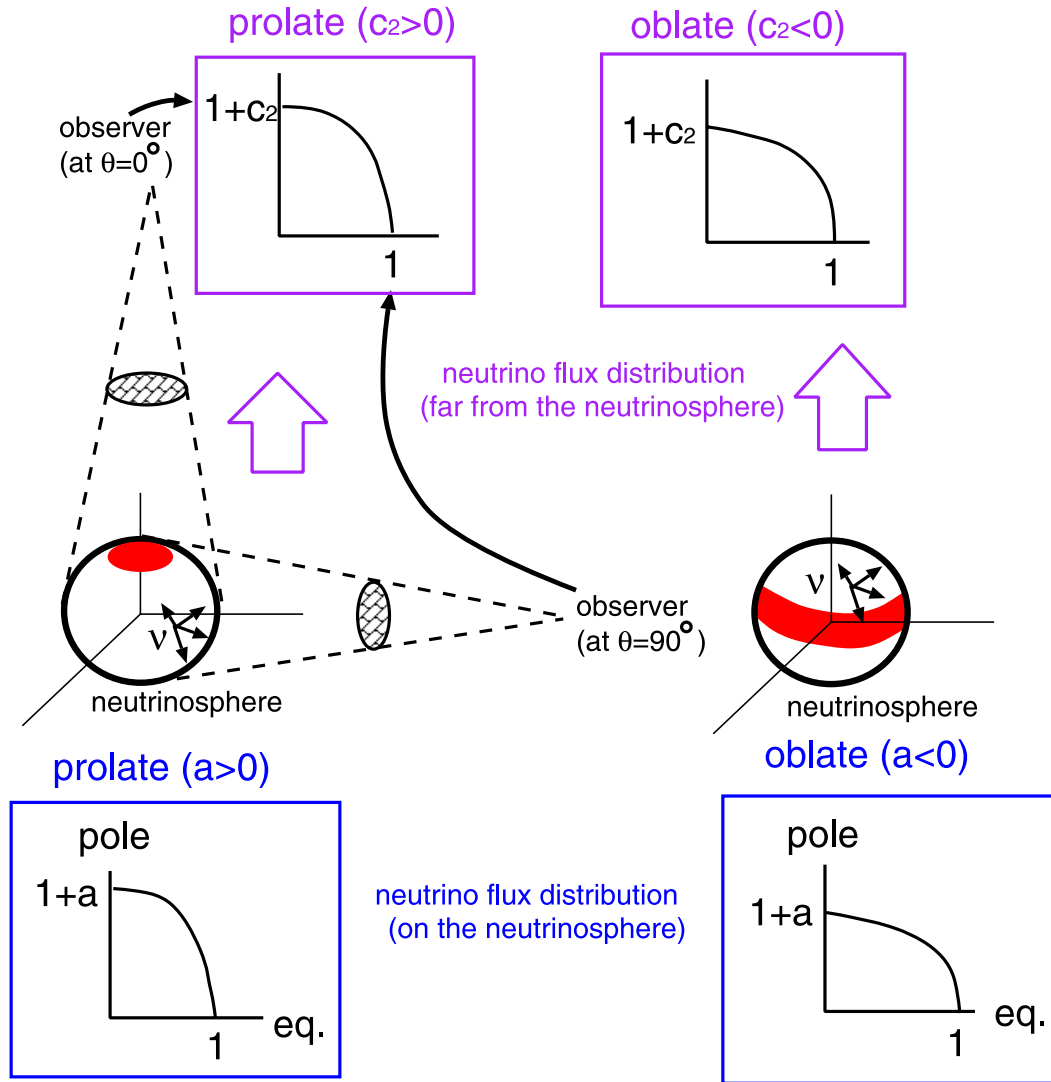


Fig. 1. Schematic picture that shows the relationship between the neutrino flux on the neutrinosphere and that for an observer far from the neutrinosphere. Due to the geometric effect from an anisotropically radiating surface, $|c_2|$ is always smaller than $|a|$.

One can easily confirm that the neutrino flux along the pole (l_z) and that on the equatorial plane (l_x) are proportional to $c_1(1 + c_2)$ and c_1 , respectively. The degree of anisotropy at a distant point far from the neutrinosphere, l_z/l_x , is then given by

$$\frac{l_z}{l_x} = 1 + c_2. \tag{5}$$

Accordingly, the neutrino flux has its maximum at the pole or on the equator when the sign of c_2 is positive or negative, respectively.

We have to emphasize that the degree of anisotropy in the neutrino flux distribution for an observer far from the neutrinosphere is different from that on the neutrino-emitting surface. This is schematically illustrated in figure 1. When we observe the neutrino flux far from the neutrinosphere, the local neutrino flux is seen as equation (1). On the other hand, the neutrino flux on the neutrino-emitting surface has a similar profile, but the degree of anisotropy is different

from equation (1). This is because a distant observer obtains the neutrino flux by integrating all of the contributions over the solid angle from an anisotropically radiating surface, and hence the degree of anisotropy is reduced for the observer (the geometric effect we call). For the neutrino flux on the neutrino-emitting surface, c_2 in equation (1) is replaced by a , where a is a parameter that represents the degree of anisotropy in the neutrino radiation on the neutrinosphere. The angular dependence of the neutrino flux on the neutrinosphere is then represented as

$$l_\nu \sim 1 + a \cos^2 \theta. \tag{6}$$

In principle, the value of c_2 is calculated from a given a by taking into account the geometric effect from an anisotropically radiating surface. Although it is difficult to calculate the exact relationship between c_2 and a , we can estimate it in a same way as in Madokoro, Shimizu, and Motizuki (2003). The neutrino flux observed far from the neutrinosphere is obtained by averaging all of the contributions from the flux on the

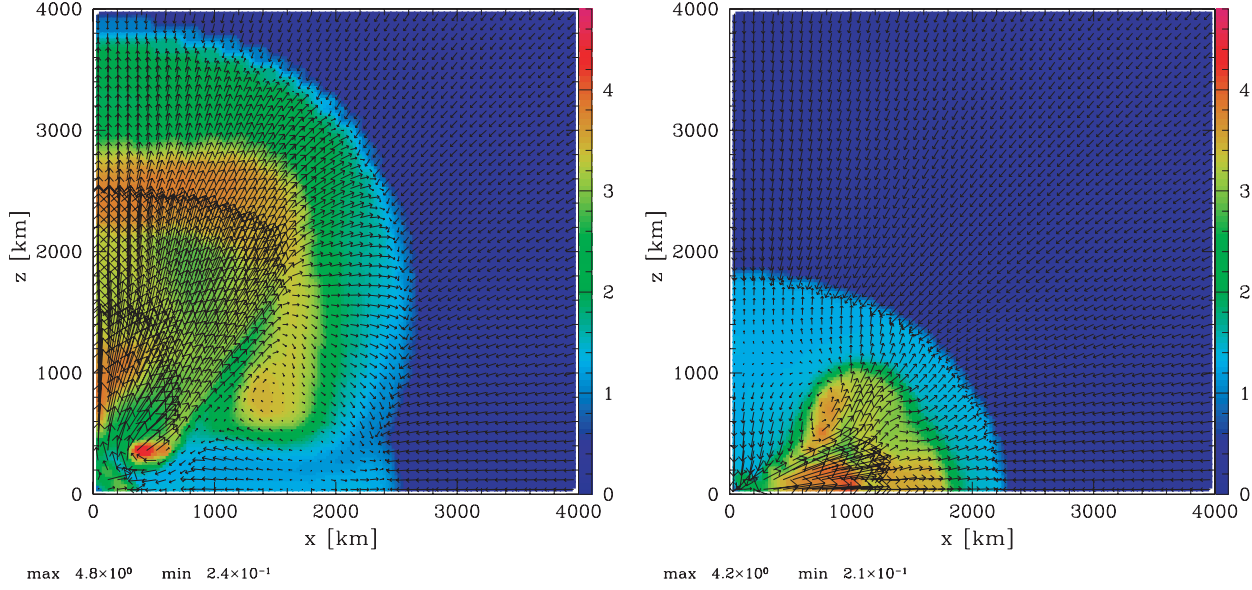


Fig. 2. Color-scale maps of the dimensionless entropy distribution and the velocity fields for the two models, pro100 (Left) and obl091 (Right), at $t \sim 280$ ms after the shock stall.

surface of the neutrino sphere. From a similar procedure to that in Madokoro, Shimizu, and Motizuki, (2003), we obtained the ratio of the local neutrino flux along the polar axis (l_z) to that on the equatorial plane (l_x) for an observer far from the neutrinosphere as a function of a ,

$$\frac{l_z}{l_x} \sim \frac{4 + 2a}{4 + a}. \quad (7)$$

By comparing equation (7) with equation (5), we finally obtained

$$c_2 \sim \frac{a}{4 + a}. \quad (8)$$

Note that equation (7) is different from equation (7) in Madokoro, Shimizu, and Motizuki (2003). This is because the profile of the neutrino flux on the neutrinosphere is approximated by a step function in Madokoro, Shimizu, and Motizuki (2003), while we directly used equation (6) to obtain (7) in this study.

3. Prolate and Oblate Explosions

We first consider prolate and oblate explosions with the same degree of anisotropy: $l_z/l_x = 1.1$ (model pro100) and $l_z/l_x = 1/1.1$ (model obl091). The values of c_2 are 0.1 and -0.091 , respectively. The spherical model (model sph000) is also examined for a comparison. The temperature on the neutrino-emitting surface, T_ν , is at first fixed to be 4.70 MeV. For models pro100, obl091, and sph000, we also considered cases with different values of the neutrino temperature ($T_\nu = 4.65$ and 4.75 MeV) in order to check the sensitivity of the results on the neutrino temperature. We further considered several cases by changing the degree of anisotropy in the neutrino radiation in order to examine at what degree of anisotropy the effect of anisotropic neutrino radiation will saturate for both the prolate and oblate models. The models that we examined are summarized in table 1.

Figure 2 depicts color-scale maps of the dimensionless entropy distribution with the velocity fields for the two models, pro100 and obl091, at $t \sim 280$ ms after the shock stall (for translation to the dimensional entropy, see Shimizu et al. 2001).

Table 1. Simulated Models.*

Model	l_z/l_x	c_2	a	T_ν (MeV)
sph000	1.00	0	0	4.70
pro050	1.05	+0.050	+0.211	4.70
pro100	1.10	+0.100	+0.444	4.70
pro150	1.15	+0.150	+0.706	4.70
pro200	1.20	+0.200	+1.000	4.70
pro250	1.25	+0.250	+1.333	4.70
pro300	1.30	+0.300	+1.714	4.70
obl048	1/1.05	-0.048	-0.182	4.70
obl091	1/1.10	-0.091	-0.333	4.70
obl130	1/1.15	-0.130	-0.462	4.70
obl167	1/1.20	-0.167	-0.571	4.70
obl200	1/1.25	-0.200	-0.667	4.70
obl231	1/1.30	-0.231	-0.750	4.70
sph000T465	1.00	0	0	4.65
sph000T475	1.00	0	0	4.75
pro100T465	1.10	+0.100	+0.444	4.65
pro100T475	1.10	+0.100	+0.444	4.75
obl091T465	1/1.10	-0.091	-0.333	4.65
obl091T475	1/1.10	-0.091	-0.333	4.75

* Note that the value of $l_z/l_x = 1 + c_2$ corresponds to the ratio of the neutrino flux along the polar axis and that on the equatorial plane for an observer far from the neutrinosphere. The value of a is calculated from equation (8).

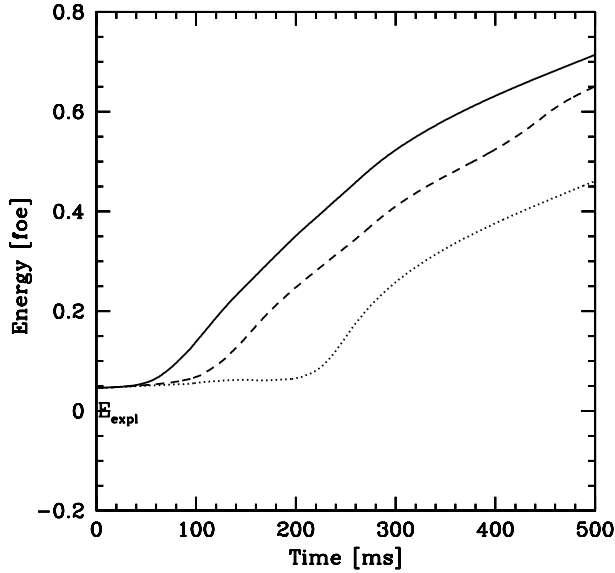


Fig. 3. Evolution of the explosion energy (E_{expl}) for model pro100 (solid line) and model obl091 (dashed line). The result of a spherical explosion, model sph000 (dotted line), for the same T_ν is also shown for a comparison.

The color boundary between dark blue and light blue shows the shock front at $r \sim 2500\text{--}3800$ km for model pro100 and at $r \sim 1800\text{--}2200$ km for model obl091. In model pro100, higher entropy upflows are mainly formed in the region of high latitudes due to intense neutrino heating on the polar axis. As the locally heated matter pushes the shock front, the shock becomes prolate and greatly distorted. On the other hand, the entropy distribution of model obl091 shows that the shock front is elongated in a oblate shape as a result of neutrino heating concentrated on the equatorial plane. We also notice that the shock front in model pro100 is clearly more extended than that in model obl091.

The evolution of the explosion energy is illustrated in figure 3. The result of the spherical model is also shown for comparison. We find that the energy gains are substantially different between the prolate and oblate models. The increase in the explosion energy is much larger in model pro100 than that in model obl091, although both models finally appear to explode.

The difference between the prolate and oblate models is attributed to the mechanism which was firstly pointed out by Shimizu et al. (2001): the importance of locally intense neutrino heating. It should be noted here that the situations of prolate and oblate explosions are different. In the former, neutrinos are predominantly emitted along the polar axis. Because of increased pressure in the locally heated matter near the pole, the shock wave is partly pushed outwards in the polar direction. The other part of the shock will follow due to the pressure gradient along the shock front. In figure 3, one can see that the explosion energy begins to increase at the position of $t \sim 40$ ms for model pro100. It is confirmed that this point corresponds to the time when the stalled shock starts to move outwards.

On the other hand, in the case of an oblate explosion, the

neutrino radiation is anisotropic, but its peak is not located point-like; the heated region is *disk-like* over the equatorial plane. The efficiency of anisotropic neutrino heating of the oblate model is considerably reduced compared with that of the prolate (local) one. This is naturally expected from the physical mechanism claimed by Shimizu et al. (2001).

Note that the neutrino heating rate, itself, is proportional to T_ν^6 , and that there are no remarkable differences in the neutrino heating rate between the prolate and oblate models. The neutrino cooling rate, however, behaves as $\sim T_m^6$, where T_m is the matter temperature. As a result of the earlier shock revival, T_m in model pro100 is quickly reduced. The neutrino cooling for the prolate model is therefore greatly suppressed with a decrease of the matter temperature during the course of the shock expansion. Thus, the explosion energy in model pro100 becomes larger than that in model obl091 (see figure 3).

Up to here, we have shown only the results of two models (pro100 and obl091) that have the same degree of anisotropy in neutrino radiation. We do not need to study many models for the prolate and oblate explosions with the same degree of anisotropy. From systematic investigations in previous papers (Shimizu et al. 2001; Madokoro et al. 2003), it has been learned that we will obtain the same result if we examine many models with various degrees of anisotropy for both the prolate and oblate neutrino radiation; a prolate explosion is always more powerful than an oblate one with the same degree of anisotropy for a given luminosity.

Next, we consider the cases in which the prolate and oblate explosions have different degrees of anisotropy. We have found that the effect of anisotropy becomes more powerful in both the prolate and oblate models as the degree of anisotropy in the neutrino radiation increases: the larger is the degree of anisotropy, the larger does the explosion energy become. It was

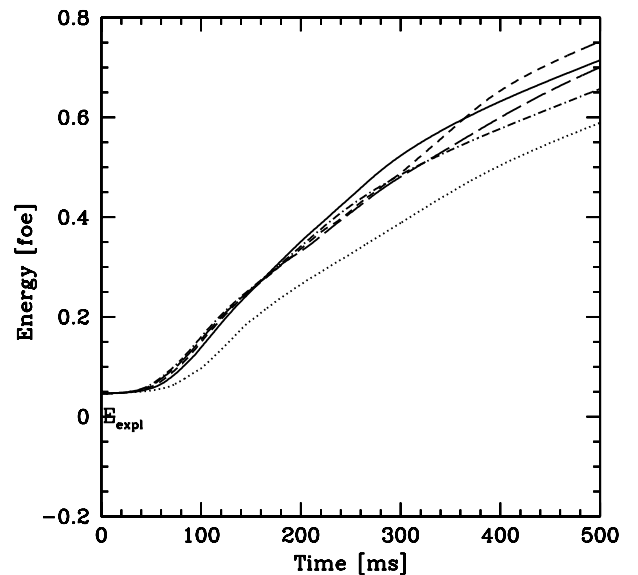


Fig. 4. Evolution of the explosion energy (E_{expl}) for the prolate models: pro050 (dotted line), pro100 (solid line), pro150 (short-dashed line), pro200 (long-dashed line), and pro250 (dot-dashed line). The result of model pro300 is close to that of model pro250, and hence we omit it.

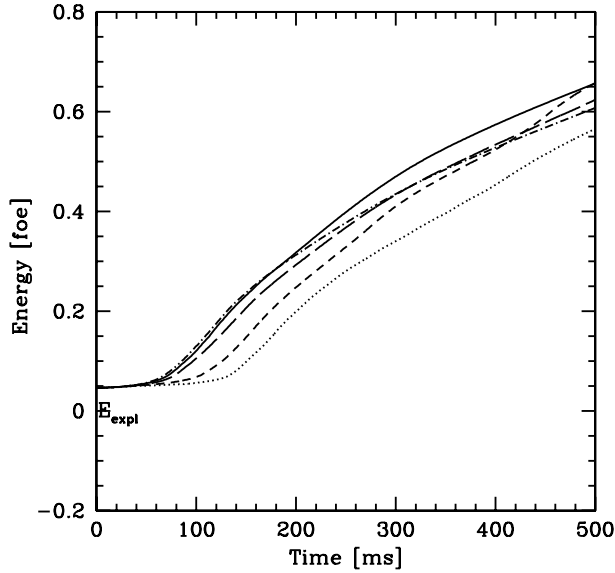


Fig. 5. Evolution of the explosion energy (E_{expl}) for the oblate models: obl048 (dotted line), obl091 (short-dashed line), obl130 (long-dashed line), obl167 (solid line), and obl200 (dot-dashed line). The result of model obl231 is close to that of model obl200, and hence we omit it.

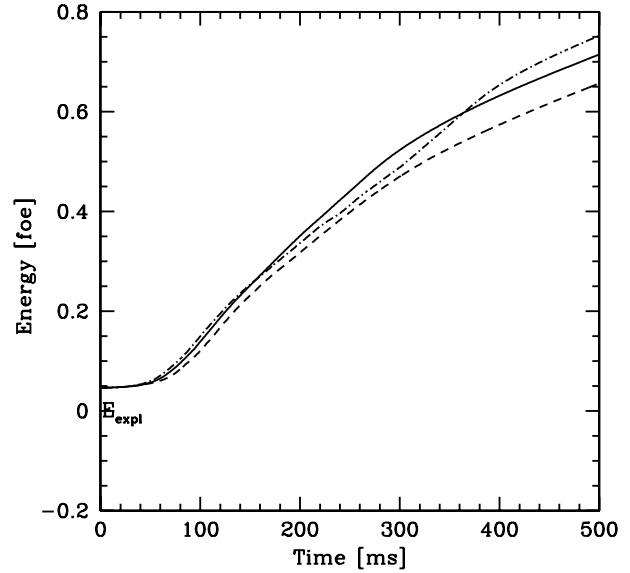


Fig. 6. Evolution of the explosion energy (E_{expl}) for the saturated models: pro100 (solid line), pro150 (dot-dashed line), and obl167 (dashed line).

found, however, that this effect saturates at around a certain degree of anisotropy [see discussion in Shimizu et al. (2001) and Madokoro et al. (2003)]. Figures 4 and 5 show the saturation properties of the anisotropic neutrino radiation for the prolate and oblate models, respectively. We can notice that, at a later stage of evolution, model pro100 ($t < 360$ ms) or pro150 ($t > 360$ ms) shows the largest explosion energy among the prolate models (figure 4), while the explosion energy of model obl167 becomes the largest among the oblate models (figure 5). This means that the saturation of the effect of anisotropic neutrino radiation appears at $l_z/l_x \sim 1.1$ – 1.15 for a prolate explosion and $l_x/l_z \sim 1.2$ for an oblate explosion. We also confirmed that the explosion energy in the prolate model of $l_z/l_x = 1.1$ is larger than that in the saturated oblate model of $l_x/l_z = 1.2$. This is explicitly illustrated in figure 6. In other words, the prolate explosion of $l_z/l_x = 1.1$ is always more energetic than any other oblate models, even if the degrees of anisotropy in oblate models become larger. We therefore conclude that a prolate explosion is generally more energetic than an oblate one for a given neutrino luminosity.

For the purpose of clarifying the sensitivity of the supernova problem on neutrino heating, we also carried out simulations of less luminous ($T_\nu = 4.65$ MeV) and more energetic ($T_\nu = 4.75$ MeV) models. When $T_\nu = 4.65$ MeV, we found that the prolate model (pro100T465) does explode, while the oblate one (obl091T465) fails. Note that the difference between 4.70 and 4.65 MeV is only 1%. In contrast, the difference between the prolate and oblate models becomes much smaller when T_ν is increased to 4.75 MeV (models pro100T475 and obl091T475). These results indicate that the effect of local neutrino heating becomes more pronounced, and therefore more important, when the total neutrino luminosity is lower.

The spherical model also finally explodes when $T_\nu = 4.70$ MeV or higher (see figure 3). This simply means that any models will explode irrespective of the degree of anisotropy if the luminosity is sufficiently high. However, we should keep in mind that the total neutrino luminosity cannot be simply increased due to the problem of small mass of the proton-neutron star and that of Ni overproduction, especially in the case of essentially spherical models (Burrows et al. 1995; Janka, Müller 1996). On the other hand, our model based on anisotropic neutrino radiation can explode at lower neutrino luminosity, and therefore could solve the problems described above.

In our previous article (Madokoro et al. 2003), we made a comparison between globally anisotropic (prolate) explosions and fluctuated explosions. We concluded in that paper that globally anisotropic neutrino radiation is more effective than the fluctuated neutrino radiation to increase the explosion energy for a given neutrino luminosity. In addition, in the present study we have found that a prolate neutrino heating produces a more energetic explosion than an oblate one. Combined with the result of Shimizu et al. (2001), we conclude that globally anisotropic (prolate) neutrino radiation is the most effective way to increase the explosion energy among various types of explosions investigated in these studies when the total neutrino luminosity is given. These results support the following statement made by Shimizu et al. (2001): globally anisotropic neutrino radiation, or locally intense neutrino heating, is of great importance to produce a successful explosion.

As we have shown, locally intense neutrino heating along the polar axis produces a robust explosion in which the shock front is deformed in a prolate form. Our results may be related to the observation that the expanding materials of SN1987A have a prolate geometry [see Wang et al. (2002) and Höflich et al. (2003)].

4. Conclusion

We performed 2-D numerical simulations of core-collapse supernova explosions with prolate and oblate neutrino radiation fields. We found that these two models give different results for the shock position at the same evolutionary stage of the explosion, the explosion energy, and the geometry of an asymmetric explosion. We also found that a prolate explosion yields a larger energy gain than an oblate one for a given neutrino luminosity. We can expect from the mechanism suggested by Shimizu et al. (2001) that a prolate explosion is more energetic than an oblate one when there is no difference of the degree of anisotropy in the neutrino radiation between these two. It is not obvious, however, whether a prolate explosion is always more powerful than an oblate one when the degree of anisotropy varies independently in these two models. Our numerical study discussed in this paper has clarified that a prolate explosion ($l_z/l_x = 1.1$) is always more powerful than oblate ones, irrespective of the degree of anisotropy.

Moreover, we found that the difference between prolate and oblate explosions becomes prominent when the total neutrino luminosity is low. This means that the local (prolate) neutrino

radiation becomes more important to increase the explosion energy as the total neutrino luminosity decreases. Owing to the problem of the small mass of the protoneutron star and that of Ni overproduction, especially in the case of essentially spherical models (Burrows et al. 1995; Janka, Müller 1996), we cannot simply increase the total luminosity to explain the observed explosion energy. Therefore, we conclude that the local (prolate) neutrino radiation is of great importance in actual supernova explosions.

One of the authors showed for the first time that locally intense neutrino heating along the axis of symmetry produces a more powerful explosion than a spherical explosion when the total neutrino luminosity is given (Shimizu et al. 2001). Our results presented in this article, together with those of our previous study (Madokoro et al. 2003), show that a prolate explosion is the most effective way to increase the explosion energy when the total neutrino luminosity is low among various types of explosions examined in these studies. Our results are suggestive of the observation that the expanding materials of SN1987A have been observed to be deformed in a prolate form [see Wang et al. (2002) and Höflich et al. (2003)].

References

- Bruenn, S. W. 1993, in *Nuclear Physics in the Universe*, ed. M. W. Guidry & M. R. Strayer (Bristol: Institute of Physics Pub.), 31
- Burrows, A., Hayes, J., & Fryxell, B. A. 1995, *ApJ*, 450, 830
- Fryer, C., Burrows, A., & Benz, W. 1998, *ApJ*, 496, 333
- Fryer, C. L., & Heger, A. 2000, *ApJ*, 541, 1033
- Fryer, C. L., & Warren, M. S. 2002, *ApJ*, 574, L65
- Herant, M., Benz, W., Hix, W. R., Fryer, C. L., & Colgate, S. A. 1994, *ApJ*, 435, 339
- Höflich, P. A., Baade, D., Khokhlov, A. M., Wang, L., & Wheeler, J. C. 2003, in *Proc. IAU Symp.*, No. 212, ed. K. A. van der Hucht, A. Herrero, & C. Esteban (San Francisco: ASP), 387
- Janka, H.-T., & Keil, W. 1998, in *Supernovae and Cosmology*, ed. L. Labhardt, B. Binggeli, & R. Buser (Basel: Institute of Astronomy), 7
- Janka, H.-T., & Mönchmeyer, R. 1989a, *A&A*, 209, L5
- Janka, H.-T., & Mönchmeyer, R. 1989b, *A&A*, 226, 69
- Janka, H.-T., & Müller, E. 1995, *Phys. Rep.*, 256, 135
- Janka, H.-T., & Müller, E. 1996, *A&A*, 306, 167
- Jeffery, D. J. 1991, *ApJ*, 375, 264
- Keil, W., Janka, H.-T., & Müller, E. 1996, *ApJ*, 473, L111
- Kifonidis, K., Plewa, T., Janka, H.-Th., & Müller, E. 2003, *A&A*, 408, 621
- Kotake, K., Yamada, S., & Sato, K. 2003, *ApJ*, 595, 304
- Leonard, D. C., Filippenko, A. V., Barth, A. J., & Matheson, T. 2000, *ApJ*, 536, 239
- Liebendörfer, M., Mezzacappa, A., Thielemann, F.-K., Messer, O. E. B., Hix, W. R., & Bruenn, S. W. 2001, *Phys. Rev.*, D 63, 103004
- Madokoro, H., Shimizu, T., & Motizuki, Y. 2003, *ApJ*, 592, 1035
- Méndez, M., Clocchiatti, A., Benvenuto, O. G., Feinstein, C., & Marraco, H. G. 1988, *ApJ*, 334, 295
- Mezzacappa, A., Calder, A. C., Bruenn, S. W., Blondin, J. M., Guidry, M. W., Strayer, M. R., & Umar, A. S. 1998, *ApJ*, 495, 911
- Miller, D. S., Wilson, J. R., & Mayle, R. W. 1993, *ApJ*, 415, 278
- Shimizu, T., Yamada, S., & Sato, K. 1994, *ApJ*, 432, L119
- Shimizu, T. M. 1995, PhD Thesis, The University of Tokyo
- Shimizu, T. M., Ebisuzaki, T., Sato, K., & Yamada, S. 2001, *ApJ*, 552, 756
- Wang, L., et al. 2002, *ApJ*, 579, 671
- Wang, L., Howell, D. A., Höflich, P., & Wheeler, J. C. 2001, *ApJ*, 550, 1030
- Wang, L., Wheeler, J. C., Li, Z., & Clocchiatti, A. 1996, *ApJ*, 467, 435
- Woosley, S. E., Wilson, J. R., Mathews, G. J., Hoffman, R. D., & Meyer, B. S. 1994, *ApJ*, 433, 229

